Total Lithium Extraction from Lithium Iron Phosphate Batteries Using Tartaric and Formic Acids: Comparative and Kinetic Study

Mineral Processing and Extractive Metallurgy Review
An International Journal

ISSN: 0882-7508 (Print) 1547-7401 (Online) Journal homepage: www.tandfonline.com/journals/gmpr20

Total Lithium Extraction from Lithium Iron Phosphate Batteries Using Tartaric and Formic Acids: Comparative and Kinetic Study

Brenda Segura-Bailón, Elodie Schneider, Jernej Jozic & Martina Petranikova

To cite this article: Brenda Segura-Bailón, Elodie Schneider, Jernej Jozic & Martina Petranikova (2025) Total Lithium Extraction from Lithium Iron Phosphate Batteries Using Tartaric and Formic Acids: Comparative and Kinetic Study, Mineral Processing and Extractive Metallurgy Review, 46:8, 921-932, DOI: 10.1080/08827508.2025.2492618

To link to this article: https://doi.org/10.1080/08827508.2025.2492618

Published online: 23 Apr 2025.

MINERAL PROCESSING AND EXTRACTIVE METALLURGY REVIEW
2025, VOL. 46, NO. 8, 921–932
https://doi.org/10.1080/08827508.2025.2492618

Taylor & Francis
Taylor & Francis Group

Total Lithium Extraction from Lithium Iron Phosphate Batteries Using Tartaric and Formic Acids: Comparative and Kinetic Study

Brenda Segura-Bailón[a], Elodie Schneider[b], Jernej Jozic[a], and Martina Petranikova[a]

[a]Department of Chemistry and Chemical Engineering, Industrial Materials Recycling and Nuclear Chemistry, Chalmers University of Technology, Gothenburg, Sweden; [b]CESI, Ecole d'ingénieurs, Nancy, France

ABSTRACT

The rapid expansion of the battery market also increases the demand for raw materials, particularly metals. Recently, new technologies have been implemented to recover valuable materials from secondary resources. In this investigation, a hydrometallurgical method for lithium iron phosphate ($LiFePO_4$, LFP) battery recycling is proposed. The effectiveness of tartaric ($C_4H_6O_6$) and formic (CH_2O_2) acids for lithium extraction was evaluated and compared. The effect of organic acid concentration, temperature, oxidant addition, and solid–liquid ratio were the parameters analyzed. This study demonstrated that both agents extract 100% of lithium. Kinetics analysis showed that lithium leaching was controlled by chemical reaction, estimated the apparent activation energies (E_a) of 42.4 kJ/mol and 38 kJ/mol for CH_2O_2 and $C_4H_6O_6$ systems, respectively. Moreover, the effect of oxidants in preventing the co-dissolution of specific impurities like iron and phosphorus, especially in formic acid solutions, has been demonstrated. The experimental conditions, 100 g/L, 0.5 M CH_2O_2, 2.5 vol% H_2O_2, 25°C, and 250 rpm, suppressed the iron and phosphorus leaching by >90%. This work presented an alternative method that operates at room temperature and employs nontoxic substances to improve recycling techniques for LFP batteries via complete lithium extraction.

KEYWORDS

Spent lithium iron phosphate (LFP) battery; complete lithium dissolution; organic acid leaching

Introduction

The current battery market offers products with low cost, high-energy density, weak self-discharge effect, and long service life, increasing their demand (Ji et al. 2023). Nevertheless, some batteries' components, especially metals, are considered critical raw materials; for example, lithium, cobalt, and phosphorus, which constitute nickel manganese cobalt (NMC), lithium cobalt oxide (LCO), and lithium iron phosphate ($LiFePO_4$, LFP) batteries (Krantz 2023).

Forecasts indicate that by 2030, the North American Battery Industry will require more than 35% purified phosphoric acid to satisfy the production of LFP batteries. Also, lithium demand is projected to increase by 30% (Fleischmann et al. 2023; Passalacqua 2023). For this reason, the recycling sector focuses on techniques capable of recovering and reincorporating valuable materials to decrease metal scarcity and encourage the circular economy (Li et al. 2024a).

Hydrometallurgical processes are widely employed for metal recovery due to their effectiveness, and nowadays, these techniques are being optimized. For example, organic acids are investigated to replace traditional reagents (mineral acids) due to their capacity to extract different metals selectively and in acceptable leaching yields (>90%) (Jing, Tran, and Lee 2024). Also, organic compounds are less corrosive and toxic and are considered eco-friendly (Kumari and Samadder 2022).

Chemically, organic acids dissolve metals by acidification and complexation. Acidification occurs when the organic species dissociates to donate a hydrogen cation (Equation 1), then the reduction of protons produces hydrogen (Equation 2), and the metal is oxidized (Equation 3). While in complexation, a ligand (from organic acid) forms coordination compounds with metals (Equation 4) (Jadhav, Sua, and Hocheng 2016; Saidan, Brown, and Valix 2012).

$$RCOOH + H_2O \leftrightarrow RCOO^- + H_3O^+ \quad (1)$$

$$2H_3O^+ + 2e^- \rightarrow H_2 + 2H_2O \quad (2)$$

$$M \rightarrow M^{2+} + 2e^- \quad (3)$$

$$nRCOO^- + M + nH_3O^+ \rightarrow (RCOO)_nM + nH_2O + n/2H_2 \quad (4)$$

In Equations 1 to 4, M indicates the metal and R the organic substituent group.

Citric acid ($C_6H_8O_7$) is one of the organic acids generally used for electronic waste treatment. In the battery recycling field, its capacity to recover lithium, cobalt, manganese, and nickel from NMC, LCO, and LFP batteries has been demonstrated (Kumar et al. 2020; Punt et al. 2021; Wang et al. 2022), also, the leaching processes have been improved when oxidants like hydrogen peroxide (H_2O_2) and temperature are employed (Li et al. 2009).

The use of organic reagents has been focused on lithium extraction because it is also considered a valuable material with potential applications in different industrial sectors, for example, ceramics and polymer production, psycho-medical

CONTACT Brenda Segura-Bailón bailon@chalmers.se Department of Chemistry and Chemical Engineering, Industrial Materials Recycling and Nuclear Chemistry, Chalmers University of Technology, Gothenburg, Sweden

pharmacy, etc (Reich et al. 2022). Natarajan, Boricha, and Bajaj (2018) proposed a method that employs acetic acid ($C_2H_4O_2$) and H_2O_2 for LCO battery processing. 100% Li was obtained with 3 M $C_2H_4O_2$, 70°C, 40 min, 20 g/L, and 7.5 vol%. The authors concluded that organic acid concentration plays an important role in system stabilization, so 3–4 M $C_2H_4O_2$ guarantees the high leaching efficiency of lithium.

In some cases, avoiding the co-dissolution of impurities (iron, phosphate, aluminum, copper, etc.) is necessary to achieve selectivity. An example is using oxalic acid ($C_2H_2O_4$). This agent (experimental conditions: 0.32 M $C_2H_2O_4$, 90°C, 10 g/L, 60 min) guaranteed an elevated lithium leaching rate (99% Li) in LFP battery processing, mitigating iron dissolution. Oxalic acid can form a solid compound with iron ($FeC_2O_{4(s)}$), allowing low extraction rates of the metal (≤5% Fe) (Chai et al. 2024).

On the other hand, tartaric ($C_4H_6O_6$) and formic (CH_2O_2) acids have recently been studied as potential leaching agents. Tartaric acid can be dissociated in $C_4H_5O_6^-$ ($pKa_1 = 3.03$) and $C_4H_4O_6^{2-}$ ($pKa_2 = 4.37$), and formic acid $HCOO^-$ ($pKa = 3.75$) promoting their interaction with some cations of copper, aluminium, iron, calcium, etc. (Cu^{2+}, Al^{3+}, Fe^{2+}, Fe^{3+}, Ca^{2+}, etc.), generates stable species (Sit et al. 2023; Tian et al. 2024).

Mahandra and Ghahreman (2021) developed a selective lithium extraction process from the spent cathode material of LFP batteries, employing CH_2O_2 as the leaching agent and hydrogen peroxide (H_2O_2) as the oxidant. With 10% pulp density, CH_2O_2/Li molar ratio of 3:23,10 vol% H_2O_2, at 30°C and 30 minutes, the leaching efficiencies were 89% Li and <0.5% Fe. While Zhao et al. (2023) achieved 97% Li using 0.5 M CH_2O_2, a liquid-to-solid ratio of 10 mL/g, 1.5–2.5% H_2O_2, at 20°C and 40 minutes. Furthermore, this method guaranteed the non-dissolution of impurities (iron, copper, aluminum, nickel, cobalt, and manganese).

Li et al. (2024b) confirmed the effectiveness of the CH_2O_2-H_2O_2 system for lithium LFP black mass leaching. With 0.8 M CH_2O_2, 50 g/L, 8 vol% H_2O_2, 60°C, and 60 min, it was possible to obtain 99% Li and 0.05% Fe. In this case, the temperature was crucial to promote lithium dissolution.

Tartaric acid leaching capacity has been studied mainly for refractory ore processing. Tian et al. (2024) reported a leaching efficiency of 85% Li from a material composed of aluminum, silicon, iron, calcium, manganese, lithium oxides, etc. The authors determined that some metallic impurities (aluminum, calcium, and iron) can affect lithium dissolution and highlighted the importance of their study.

In battery recycling, tartaric acid has been used primarily for NMC and LCO batteries processing, where leaching efficiencies from nickel, manganese, and cobalt are >80% (He et al. 2016; Wang, Tang, and Shen 2022; Wang et al. 2023). In particular, the efforts have been focused on cobalt extraction to generate purified products (Wang et al. 2023). Nevertheless, the study of $C_4H_6O_6$ on lithium and metallic impurities extraction from other types of batteries should be extended. Therefore, this work proposes tartaric acid application for LFP black mass treatment. The objective is to develop a green method for the selective leaching of lithium from phosphorus and iron.

In this study, tartaric and formic acids are employed as leaching agents, eco-friendly reductants capable of extracting lithium from multimetallic materials. Achieved selective leaching lowers the number of separation steps needed for elements recovery, generates non-hazardous streams and thus allows more versatile utilization of the by-products. A comparative study is presented, evaluating reagents concentration, temperature, oxidant (H_2O_2) addition, and the solid–liquid ratio. Furthermore, this work analyzes the effect of copper, iron, phosphorus, and aluminum on lithium extraction.

Materials and methods

Chemical analysis

A black mass sample with a particle size of <250 µm, provided by Stena Recycling AB Company (Sweden), was analyzed chemically. The sample was crushed and mechanically separated (Stena Recycling AB). Afterward, exactly 0.1 g of solid was digested (in triplicate) using aqua regia prepared with hydrochloric acid (HCl, 37%, Sigma-Aldrich) and nitric acid (HNO_3, 65–67%, Sigma-Aldrich) (HCl: HNO_3 3:1 v/v) at 80°C, 5 h, and 200 rpm (magnetic agitation). The solutions were cooled, filtered, and diluted to 100 mL with 0.1 M HNO_3 (65–67%, Sigma-Aldrich). To determine the chemical composition, all samples were analyzed using Inductively Coupled Plasma Optical Emission Spectroscopy (ICP-OES, Thermo Fisher Scientific, Model iCAPTM 6000 Series), where analytical grade standards (inorganic venturesTM) were used to build the calibration curves.

Leaching process

The black mass sample was leached, employing tartaric acid ($C_4H_6O_6$, 99%, Sigma-Aldrich) and formic acid (CH_2O_2, 98%, Acros organics) solutions. The tested parameters were 0.15, 0.25, and 0.5 M of leaching agent, a solid–liquid ratio of 20, 50, and 100 g/L, oxidant addition (hydrogen peroxide, H_2O_2, 50–60%, Nouryon), and temperatures of 25°C, 40°C, and 60°C. All the experiments were performed (in triplicate) using a glass reactor (100 mL, pyrex) and magnetic agitation (250 rpm). The pH was monitored employing a MeterLab (PHM240) electrode. The samples were filtered, diluted with 0.1 M HNO_3 (65–67%, Sigma-Aldrich), and analyzed by ICP-OES (Thermo Fisher Scientific, Model iCAP^{TM} 6000 Series).

Solid characterization

The original and untreated black mass sample, as well as the solid residue after the leaching process, were analyzed by X-ray diffraction technique (XRD). XRPD Siemens D5000 diffractometer was used, which operated with a radiation source in a 2θ interval of 10°–70° (Cu λ = 1.54 Å), a rotational speed of 15 rpm, and a voltage of 40 mA and 40 kV. EVA software and the JCPDS database were used for analytical interpretation.

Results and discussion

Effect of leaching agent concentration on metal extraction

Tartaric ($C_4H_6O_6$) and formic (CH_2O_2) acids were employed for processing a black mass sample whose metal composition is

Table 1. Average metallic content of the black mass sample (<250 µm).

Element	Fe	P	Li	Cu	Al	Co	Mn	Ni
wt%	13.11 ± 0.25	8.04 ± 0.16	1.81 ± 0.03	2.82 ± 0.06	1.21 ± 0.04	0.060 ± 0.001	ND	0.320 ± 0.012

ND: no detected

shown in Table 1. The tested concentrations were 0.15, 0.25, and 0.5 M, respectively, employing 20 g/L and room temperature (25°C).

Figure 1 shows the leaching efficiency for phosphorus, iron, copper, aluminum, and lithium. In the first case, by using 0.15 M of tartaric acid (Figure 1(a)). All metals (except copper) were extracted entirely after 20 minutes. The copper leaching rate was slower, but after 60 minutes, 100% of copper was extracted. In this system, the increase in tartaric concentration at 0.25 M did not represent a significant effect on metal extraction (Figure 1(c)). Nevertheless, with higher concentration (0.5 M $C_4H_6O_6$, Figure 1(e)), shows that copper dissolution decreased significantly after 30 minutes. This phenomenon can be associated with tartaric acid concentration. If $C_4H_6O_6$ is in excess amounts relative to copper content, an insoluble compound can be formed in acid media ($CuC_4H_6O_{6(s)}$) (Gyliené, Salkauskas, and Juskénas 1997; Pan et al. 2024).

Notable differences are observed with the formic acid system (Figure 1(b)). Firstly, lithium and aluminum were completely dissolved after 30 minutes, and the extraction reached equilibrium. The leaching efficiency of copper increased to 100% despite its slower leaching kinetics than aluminum and lithium. Copper dissolution is linked to copper oxide species ($CuO_{(s)}$) found as impurities in the black mass sample (Figure A1, Appendix), allowing the chemical interaction between copper ions and the ionized formic acid radical ($Cu[HCOO]^+$, Log K at 25°C = 2.0, Puigdomenech 2004). Finally, the yield of phosphorus and iron decreased in the first minutes and behaved similarly during the 120 minutes. This tendency was also observed in Figure 1(d,f); however, the phosphorus and iron leaching kinetics were slower compared to Figure 1(b). This behavior is associated with the presence of iron(III) phosphate salt ($FePO_{4(s)}$, Log K at 25°C = 26.4 (Puigdomenech 2004), in the leaching system.

It is important to highlight that the pH of the tested solutions was not adjusted, and its value was relatively constant (pH ~ 2) throughout the experiments in all chemical systems. On the other hand, the previous analysis demonstrated that both leaching agents guarantee lithium extraction, which is not affected despite the dissolution of copper and aluminum. Furthermore, the effect of temperature was studied to comprehend the lithium leaching efficiency in both chemical systems.

Effect of temperature on lithium leaching efficiency

Experimental tests were performed at 40°C and 60°C, employing 0.5 M of $C_4H_6O_6$ and CH_2O_2, respectively (Figure 2). The tartaric acid system (Figure 2(a)) allowed the extraction of all metals in a short time (<20 min); however, this system did not improve the lithium, copper, and aluminum extraction, which leaching efficiency decreased by 85% Li, 77% Cu, and 82% Al, compared to the previous systems (Figure 1). Otherwise, iron and phosphorus leaching efficiency was 70% and 80%, respectively, values lower than reported in Figure 1(e) but higher compared to the CH_2O_2 system.

On the other hand, in the formic acid solution (Figure 2(b)), the leaching yield of iron and phosphorus improved compared with the prior case (Figure 1(f)). However, the experimental conditions did not allow lithium, copper, and aluminum dissolution; the leaching efficiency was 83% Li, 70% Cu, and 82% Al.

At 60°C with $C_4H_6O_6$ (Figure 3(a)), the leaching efficiency for all metals enhanced compared to Figure 2(a). In contrast, in the second system, CH_2O_2, even though the iron and phosphorus leaching efficiency was ~30%, lithium extraction was not favored, obtaining ~70% of lithium (Figure 3(b)).

Increasing the temperature is convenient for a short time: ≤30 minutes for the $C_4H_6O_6$ system and ≤5 minutes for CH_2O_2 to accomplish the complete lithium extraction. Nevertheless, all impurities are extracted above 50% in tartaric acid solutions. Although the formic acid system achieved efficiencies lower than 50%, especially iron and phosphorus, are similar to results at room temperature (Figure 1).

Effect of hydrogen peroxide (H_2O_2) in solutions of tartaric ($C_4H_6O_6$) and formic (CH_2O_2) acid

The influence of hydrogen peroxide (H_2O_2) as an oxidant was evaluated in the chemical systems. H_2O_2 was selected because it is considered one of the most powerful and clean oxidizing agents widely employed in ores and battery treatment (Li et al. 2009; Nicol 2020). The function of H_2O_2 and CH_2O_2 is to enhance lithium extraction, allowing Li^+ to be released from the solid material while $FePO_{4(s)}$ remains as a residue (Li et al. 2024b; Mahandra and Ghahreman 2021).

The effect of H_2O_2 was tested in the systems with lower and higher concentrations of organic agent (0.15 M and 0.5 M, respectively) at 25°C and under acid conditions (pH ~ 2) like the systems described above. Figure 4(a) shows the results in $C_4H_6O_6$-H_2O_2 solutions. In the system with 0.15 M $C_4H_6O_6$, aluminum and lithium were extracted completely, and the leaching efficiency of phosphorus, copper, and iron was 92.5%, 60%, and 73%, respectively. The decrease in iron and copper leaching yield is because not only Cu^{2+} but also Fe^{2+} and Fe^{3+} react to tartaric acid and forming insoluble compounds ($Fe_2(C_4H_4O_6)_{3(s)}$, $\mathrm{Log K(25°C)} = 9.8$ and $FeC_4H_4O_{6(s)}$, $\mathrm{Log\ K(25°C)} = 2.6$, Paris and Desboeufs 2013; Tian et al. 2024). A similar behavior is observed when the concentration of tartaric acid increased to 0.5 M (Figure 4(b)), this compound reacted preferentially with copper promoting its precipitation ($CuC_4H_4O_{6(s)}$, $\mathrm{Log\ K(25°C)} = 3.20$, (Simeon, Voloder, and Weber 1969); meanwhile, the leaching of the other metals remained unaffected. This

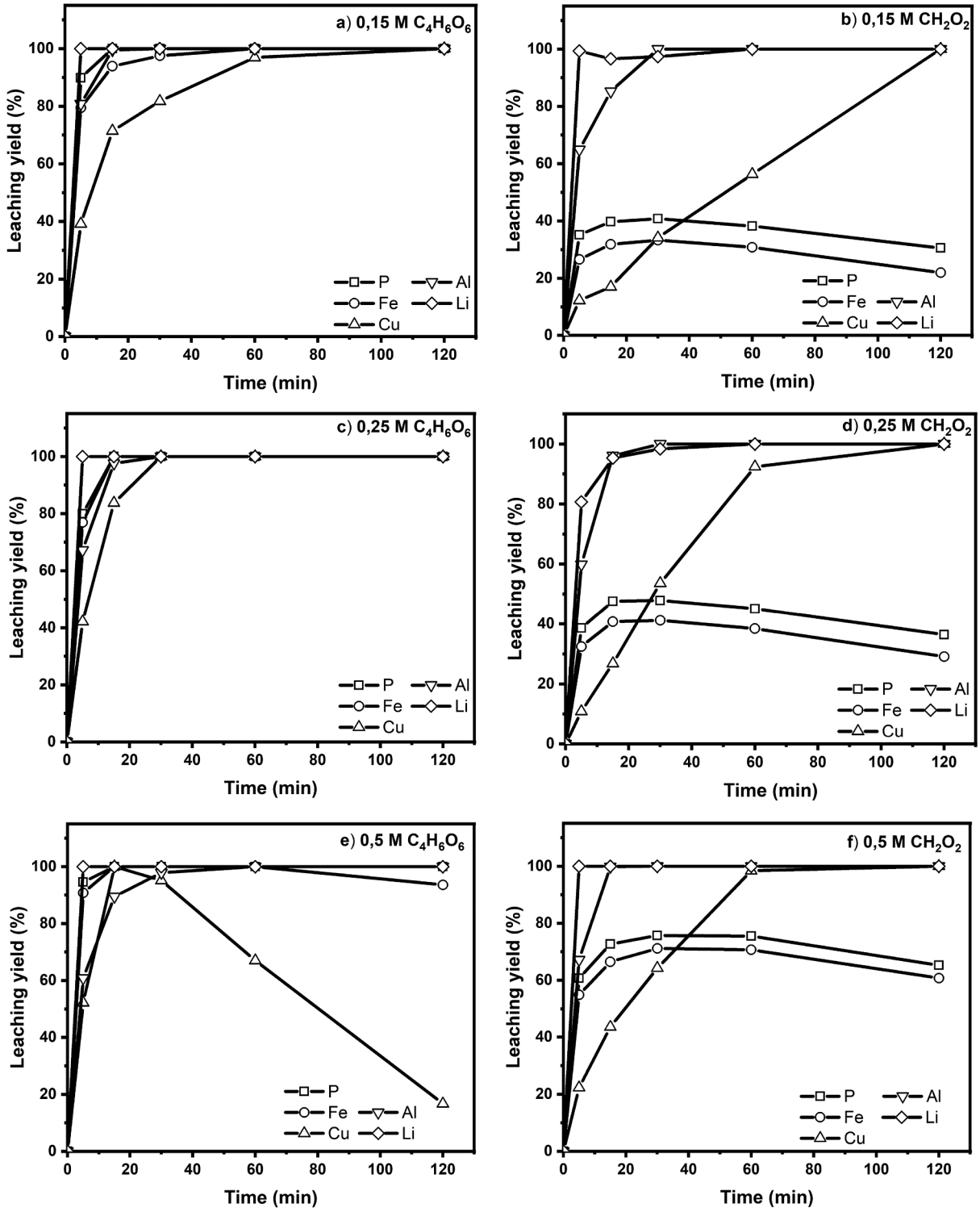

Figure 1. Leaching efficiency. Experimental conditions: 20 g/L, 25°C, 250 rpm, with different concentrations of $C_4H_6O_6$ and CH_2O_2 (0.15, 0.25, and 0.5 M).

behavior is consistent with the results shown in Figure 1(e).

On the other hand, the inhibition of iron and phosphorus leaching enhanced in the CH_2O_2-H_2O_2 system. 12% P and <2% Fe was obtained with 0.15 M CH_2O_2 (Figure 5(a)), and 12% P and ~2% Fe when 0.5 M CH_2O_2 was used (Figure 5(b)). All lithium, copper, and aluminum leaching were achieved in both cases. Although the longer leaching time compared to the systems in Figure 1, lithium, phosphorus, aluminum, and iron leaching efficiency remained constant throughout the testing time.

The results in Figures 4 and 5 demonstrated that hydrogen peroxide is essential for minimizing the co-dissolution of iron and phosphorus, particularly iron, the predominant metal in the black mass sample (Table 1). This benefits the formation of $FePO_{4(s)}$ in formic acid media and does not

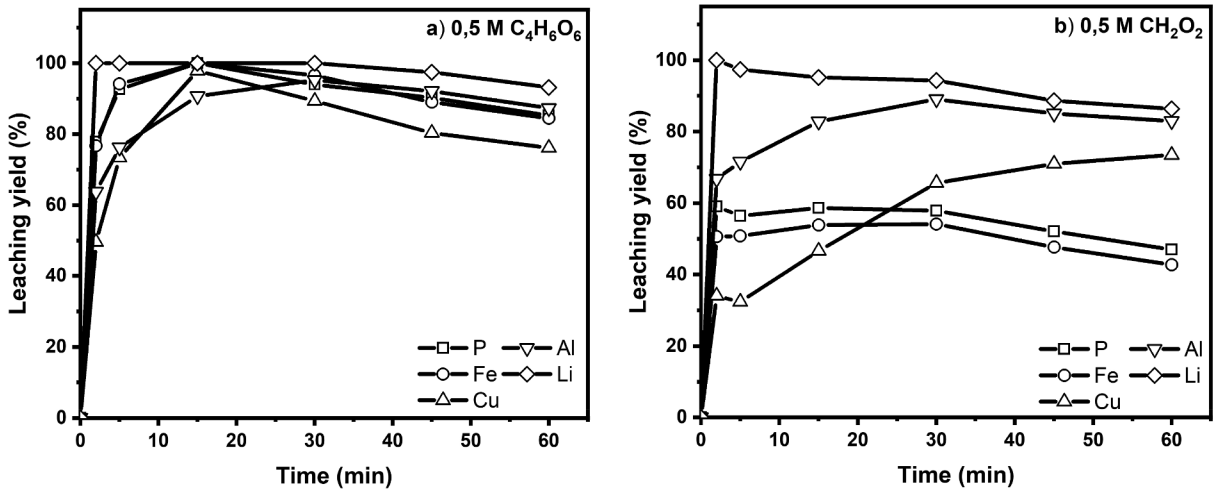

Figure 2. Leaching efficiency. Experimental conditions: (a) 0.5 M $C_4H_6O_6$ and (b) 0.5 M CH_2O_2, with 20 g/L, 40°C, and 250 rpm in both cases.

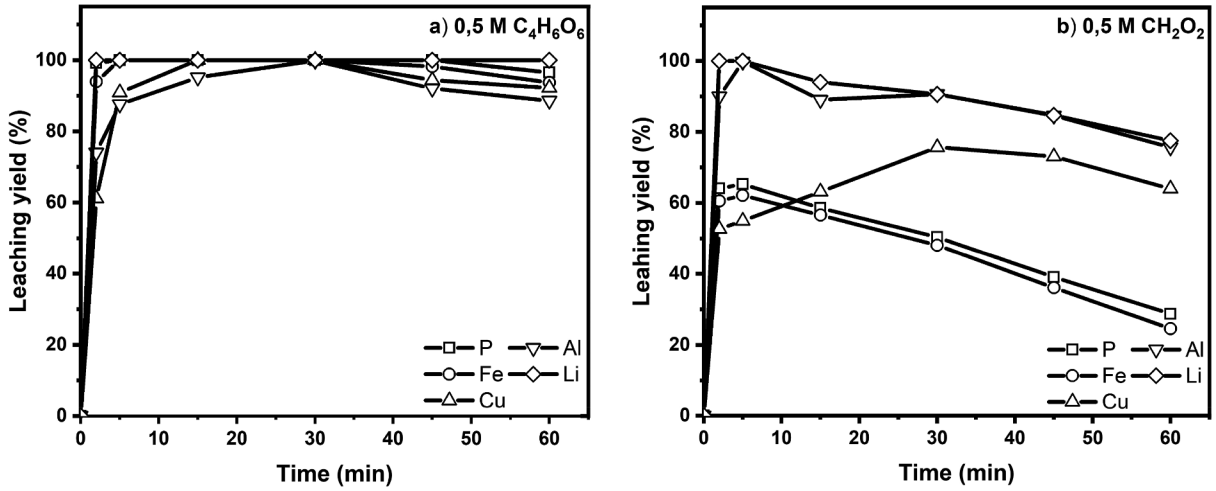

Figure 3. Leaching efficiency. Experimental conditions: (a) 0.5 M $C_4H_6O_6$ and (b) 0.5 M CH_2O_2, with 20 g/L, 60°C, and 250 rpm in both cases.

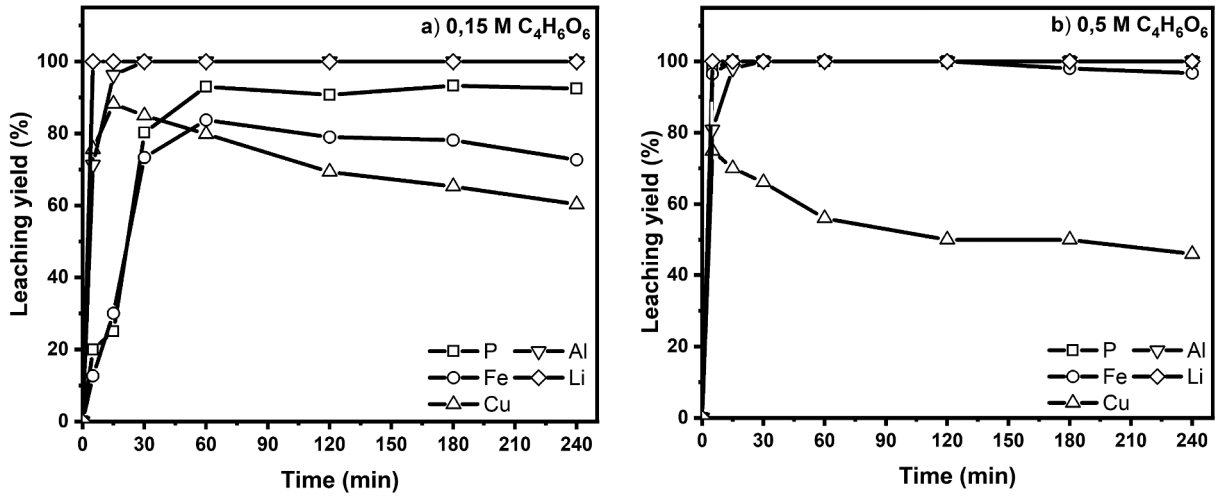

Figure 4. Leaching efficiency. Experimental conditions: (a) 0.15 M $C_4H_6O_6$ and (b) 0.5 M 0.5 M $C_4H_6O_6$, with 20 g/L, 25°C, 250 rpm and 2.5 vol% H_2O_2 in both cases.

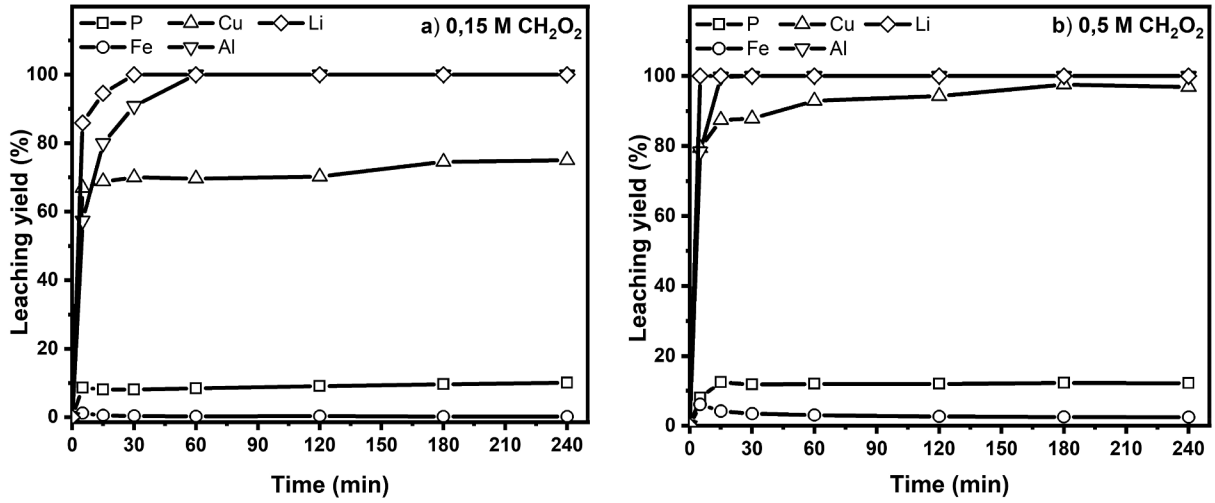

Figure 5. Leaching efficiency. Experimental conditions: (a) 0.15 M CH_2O_2 and (b) 0.5 M CH_2O_2, with 20 g/L, 25°C, 250 rpm and 2.5 vol% H_2O_2 in both cases.

negatively affect lithium extraction. Furthermore, 2.5 vol% H_2O_2 guaranteed an acceptable lithium dissolution. Some works (Li et al. 2024b; Mahandra and Ghahreman 2021) reported that hydrogen peroxide in formic acid solutions should be less than 10 vol% to favor ferric phosphate formation. Therefore, with the established experimental criteria, the effect of the solid–liquid ratio in the CH_2O_2 -H_2O_2 system was studied.

Effect of solid–liquid ratio in formic acid-hydrogen peroxide (CH_2O_2-H_2O_2) system

The tests were performed employing 0.5 M CH_2O_2 at 25°C, 2.5 vol% H_2O_2, and two solid–liquid ratios of 50 and 100 g of black mass per liter of solution. The highest leaching agent concentration guarantees enough $HCOO^-$ in the system.

In both chemical systems (Figure 6), the lithium leaching efficiency was 100% after 30 minutes. Aluminium and copper were also completely dissolved, despite the copper leaching kinetics being slower in the second system (Figure 6(b)). Regardless of the solid–liquid ratio, iron and phosphorus leaching efficiency was 0.1% Fe and 10%, indicating that phosphorus was inhibited above 90% and iron completely. Thus, the optimal experimental conditions were 0.5 M CH_2O_2, 100 g/L, 2.5 vol% H_2O_2, and 25°C.

In the chemical systems described above, the pH increased from ~2 to ~6; this variation is directly related to insoluble iron compounds formation. According to the species distribution diagram (Figure 7(a)), $FePO_{4(s)}$ (Log K at 25°C = 26.4, Puigdomenech 2004) is predominant in a pH interval of 1 to ~6. However, a second compound ($Fe(OH)_{3(am)}$, Log K at 25°C = −4.8, Puigdomenech 2004) can be formed. Finally, XRD analysis was conducted to determine the species in the solid leaching residue. Figure 7(b) confirmed the presence of ferric phosphate ($FePO_{4(s)}$) and graphite as the remaining materials.

Kinetic study of the leaching process

The Shrinking-Core Model (SCM) was considered to describe the leaching kinetics in the studied systems (tartaric and formic acids without oxidant addition at 25°C,

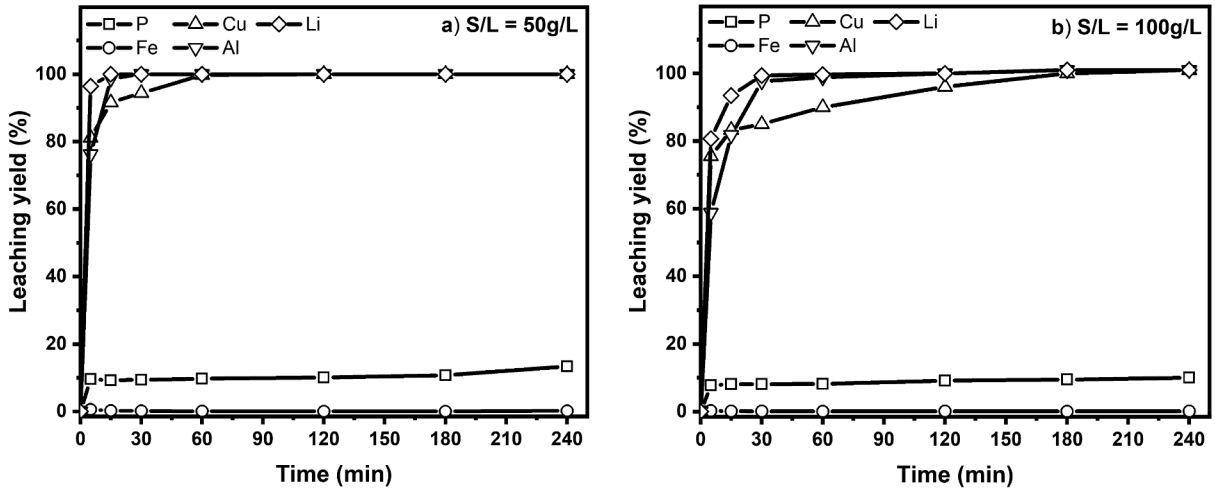

Figure 6. Leaching efficiency. Experimental conditions: 0.5 M CH_2O_2, 25°C, 250 rpm, 2.5 vol% H_2O_2, with 50 g/L (a) and 100 g/L (b).

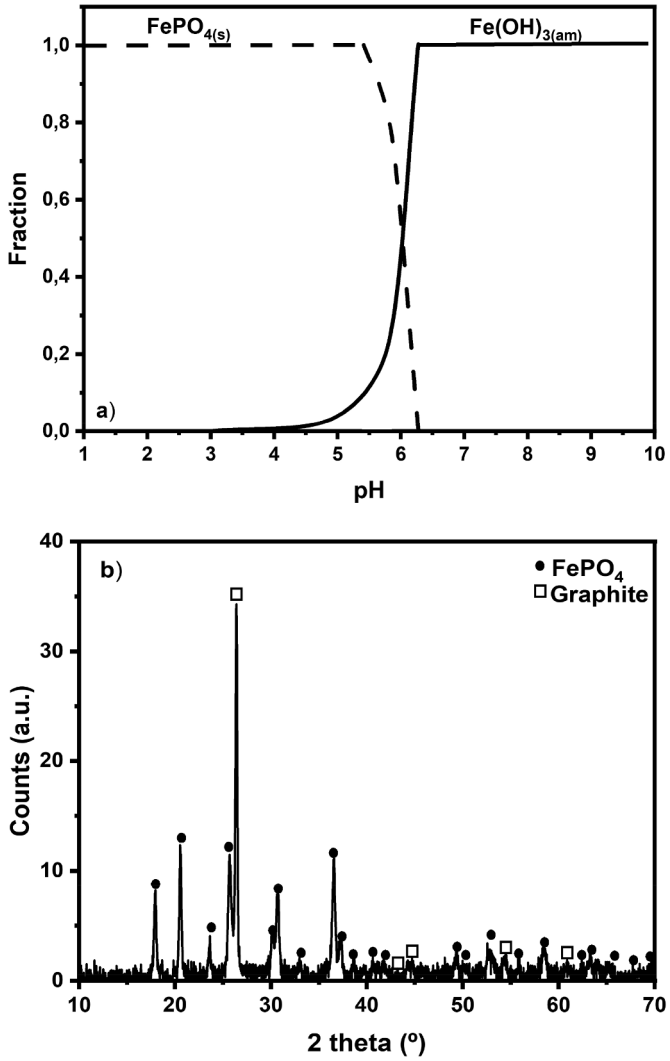

Figure 7. (a) Species distribution diagram: Fe-PO_4^{3-}. Elaborated using make equilibrium diagrams using sophisticated algorithms (MEDUSA) software (Puigdomenech 2004). (b) Solid residue (after leaching with 100 g/L, 0.5 M CH_2O_2, 2.5 vol% H_2O_2, 25°C, and 250 rpm) diffractogram.

40°C, and 60°C). SCM proposes that the chemical reaction initially occurs at the particle's external surface. The reaction zone then progresses inward, shrinking the core until the chemical reaction concludes. This model suggests that chemical reaction or mass transfer phenomena can control the leaching process. Moreover, criteria like spherical particles and the Stokes regime are assumed (Levenspiel 1999). The results of this work were consistent with the SCM-chemical reaction control (Equation 5).

$$\left[1-(1-X_B)^{1/3}\right]=\frac{bk''{C_{A_L}}^n}{\rho_B R_o}t \quad (5)$$

where X_B is the fractional conversion of solid material, b stoichiometric coefficient of solid specie, k″ the first-order rate constant for the surface reaction, C_{A_L} the concentration of liquid-phase reactant, n number of moles, ρ_B molar density (solid), R_o average particle size, and t, time. Equation (5) can be represented graphically as $\left[1-(1-X_B)^{1/3}\right]$ as a function of time (t), where $\frac{bk''{C_{A_L}}^n}{\rho_B R_o}$ corresponds to the slope (m) of the linear equation.

Lithium, iron, and copper leaching data fits linearly with the proposed model in both chemical systems ($R^2 > 0.90$, Figure 8). However, P-CH_2O_2 and Al-CH_2O_2 data did not fit appropriately ($0.85 > R^2 \leq 0.90$). In all cases, the slope becomes steeper as the temperature rises, indicating that the fractional conversion is directly related to the temperature effect. Furthermore, the SCM was applied for a short period, implying that in ≤60 minutes, the process was controlled by the chemical reaction.

Arrhenius equation (Equation 6) was used to determine the apparent activation energy (E_a) in metal-organic acid systems.

$$k(T)=A^{-E_a/RT} \quad (6)$$

Equation (6) describes the dependence between the reaction rate constant (k) and temperature, where A is the frequency factor, R is the gas constant (8.314 J/molK), and T is the absolute temperature (K). Arrhenius expression can also be represented as a linear form (ln(k) as a function of 1/T). Therefore, E_a is estimated from the plot data ($m = E_a/R$) (Ancheyta 2017).

The estimated E_a values (based on the information in Figure 9) for lithium, phosphorous, iron, copper, and

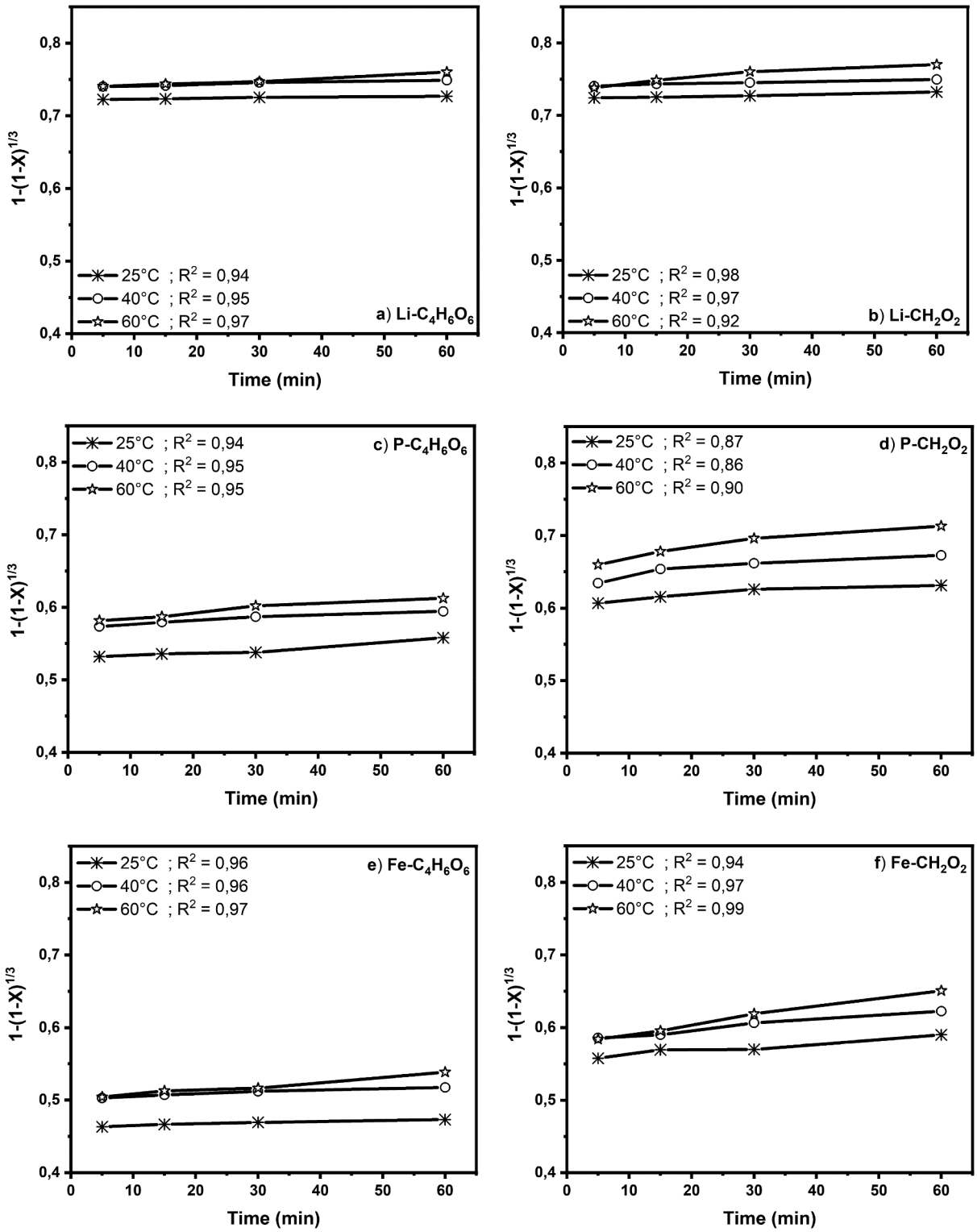

Figure 8. Shrinking-core model adjusted data. Metal-organic acid systems (leaching experimental conditions: 0.5 M $C_4H_6O_6$ or CH_2O_2, with 20 g/L and 250 rpm).

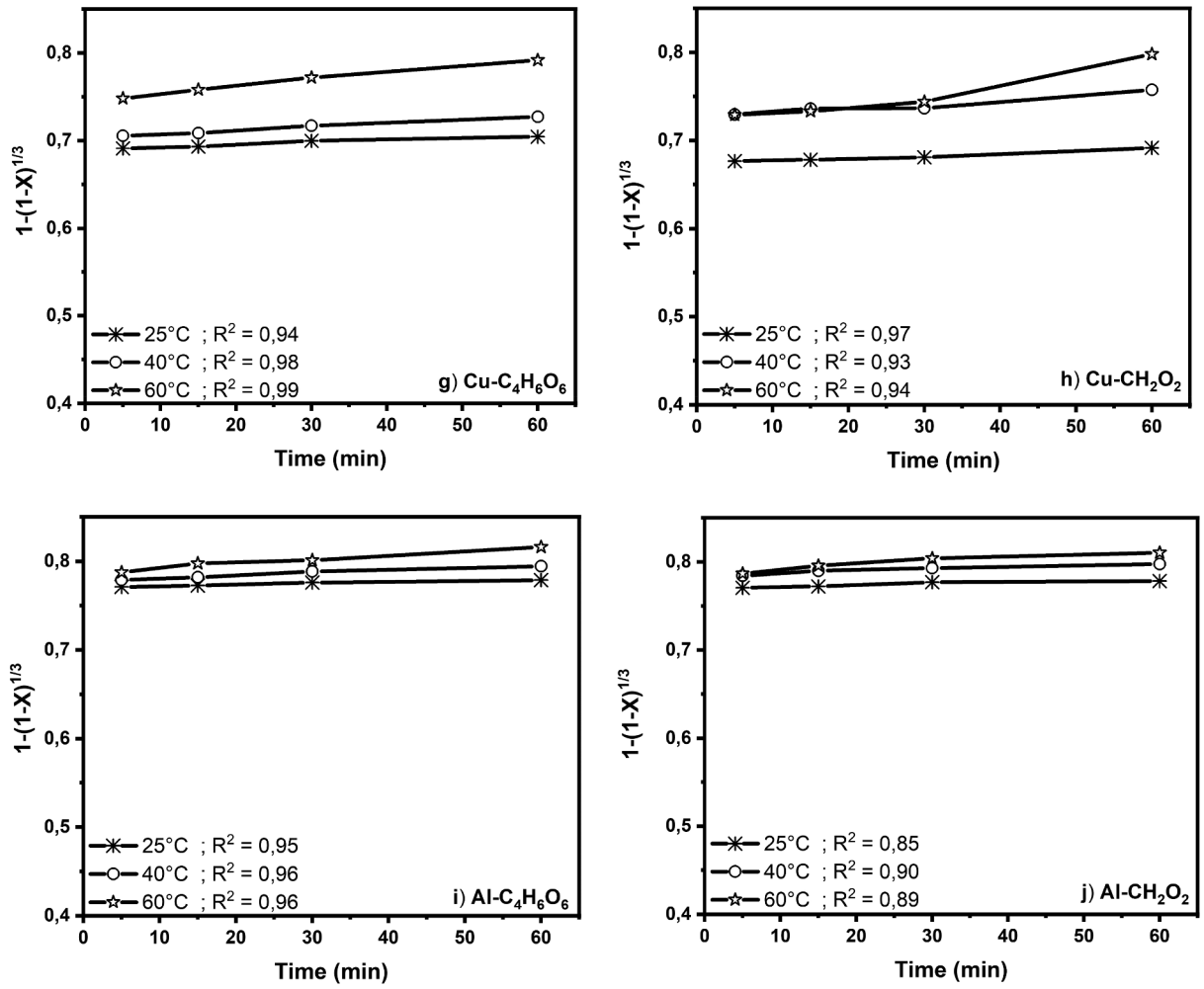

Figure 8. (Continued).

aluminium in the formic acid system were 42.4, 19.3, 20.7, 34.8, and 38 kJ/mol, while the values in tartaric acid were 38, 16.4, 26.1, 23.4, and 37.5 kJ/mol for lithium, phosphorous, iron, copper, and aluminium, respectively. The results indicate that lithium and aluminium followed the chemical reaction-controlled process; however, the values for the other metals did not correlate suitably. For that reason, kinetic analysis must be enhanced; for example, using modified shrinking-core models could improve the estimation of apparent activation energy.

Conclusions

A method for lithium extraction from LFP black mass was presented. The study focused on analyzing the effectiveness of tartaric and formic acid as organic leaching agents. Both reagents could successfully extract 100% of lithium at room temperature. Nevertheless, other metals such as iron, phosphorus, aluminum, and copper were also dissolved, and their dissolution improved in $C_4H_6O_6$ solutions when the temperature increased (40°C and 60°C), while all metals, including lithium, precipitated in the CH_2O_2 system, negatively impacting the extraction.

When hydrogen peroxide was employed as an oxidant, it benefited the inhibition of phosphorus and iron, mainly in formic acid solutions, in more than 90%. So, the experimental conditions 100 g/L, 0.5 M CH_2O_2, 2.5 vol% H_2O_2, 25°C, and 250 rpm promoted the formation of an insoluble compound, $FePO_{4(s)}$, without affecting lithium leaching efficiency. Therefore, the CH_2O_2+H_2O_2 system positively influenced the entire lithium extraction from the black mass sample. On the other hand, a kinetic perspective of the leaching process was presented, where the apparent activation energy values (E_a = 42.4 kJ/mol for Li-CH_2O_2 and E_a = 38 kJ/mol for Li-$C_4H_6O_6$) determined that lithium extraction is directly related to chemical reaction-control.

Finally, this method illustrates that organic compounds can effectively allow complete extraction of lithium, achieving leaching rates comparable to mineral acids. Therefore, these organic species are considered an alternative route for spent battery treatment, highlighting the importance of using organic, nontoxic, and eco-friendly substances and processes that can operate at room temperature, contributing to developing more sustainable methods.

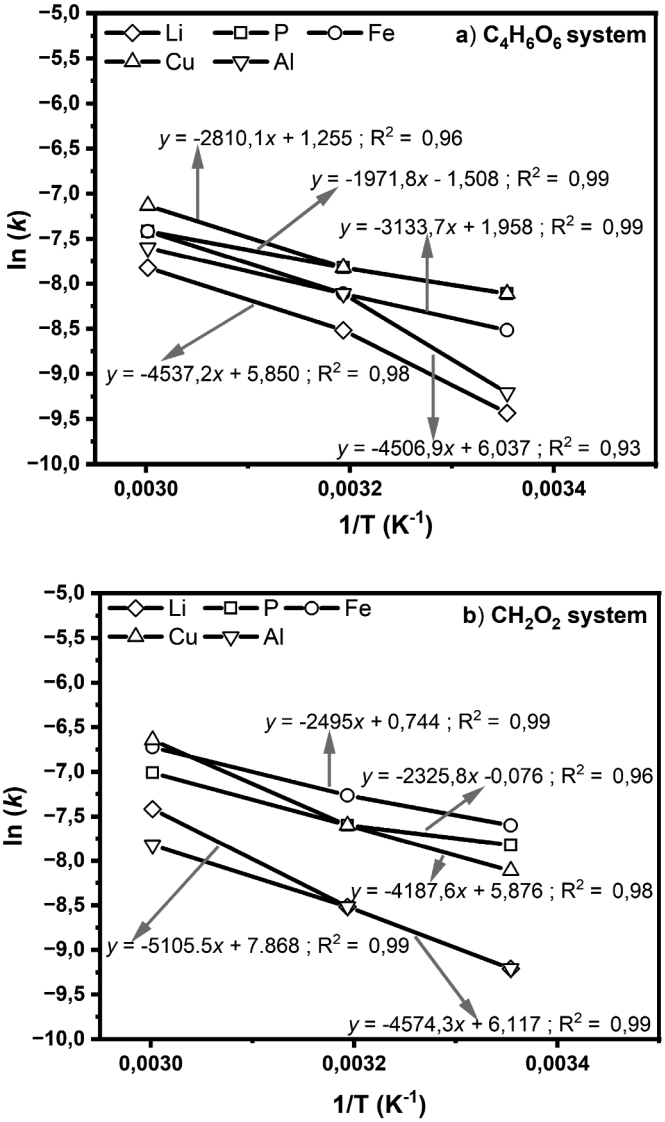

Figure 9. Arrhenius equation fitting. Metal-organic acid systems (leaching experimental conditions: 0.5 M $C_4H_6O_6$ or CH_2O_2, with 20 g/L and 250 rpm).

Acknowledgments

The authors thank the Swedish Energy Agency [Grant number: P2022-00077], BASE (Batteries Sweden) by Vinnova [Grant No. 2019-00064], and Stena Recycling International AB [Project number 21290041] for financial support and for providing the black mass sample.

Disclosure statement

No potential conflict of interest was reported by the author(s).

Funding

This work was supported by Stena Recycling International AB [Project No. 21290041], BASE (Batteries Sweden) by Vinnova [Grant No. 2019-00064], and Swedish Energy Agency [Project No. P2022-00077].

References

Ancheyta, J. 2017. *Chemical reaction kinetics: Concepts, methods and case studies*. Hoboken, NJ: John Wiley & Sons Ltd.

Chai, X., X. Yu, Q. Shen, X. Li, X. Lin, W. Cai, and Y. Yuan. 2024. Study on green closed-loop regeneration of waste lithium iron phosphate based on oxalic acid system. *Waste Management* 181:168–75. doi: 10.1016/j.wasman.2024.03.037.

Fleischmann, J., P. Schaufuss, M. Linder, M. Hanicke, E. Horetsky, S. Jautelat, L. Torscht, and A. Rijt. 2023. Battery 2023: Resilient, sustainable, and circular. Accessed October 2024. https://www.mckinsey.com/industries/automotive-and-assembly/our-insights/battery-2030-resilient-sustainable-and-circular#/.

Gyliené, O., M. Salkauskas, and R. Juskénas. 1997. The use of organic acids as precipitants for metal recovery from galvanic solutions. *Journal of Chemical Technology & Biotechnology* 70 (1):111–15. doi: 10.1002/(SICI)1097-4660(199709)70:1<111::AID-JCTB691>3.0.CO;2-9.

He, L., S. Sun, Y. Mu, X. Song, and G. Yu. 2016. Recovery of lithium, nickel, cobalt, and manganese from spent lithium-ion batteries using L-Tartaric acid as a leachant. *ACS Sustainable Chemistry & Engineering* 5 (1):714–21. doi: 10.1021/acssuschemeng.6b02056.

Jadhav, U., C. Sua, and H. Hocheng. 2016. Leaching metals from large pieces of printed circuit boards using citric acid and hydrogen peroxide. *Environmental Science and Pollution Research International* 23 (23):24384–92. doi: 10.1007/s11356-016-7695-9.

Ji, W., H. Li, W. Li, Z. He, and J. Zhao. 2023. Novelty method based on thermal tigger mechanism for high energy density lithium-ion battery

safety. *Journal of Energy Storage* 64:107231. doi: 10.1016/j.est.2023.107231.

Jing, C., T. T. Tran, and M. S. Lee. 2024. A review on the recovery of lithium and iron spent lithium iron phosphate batteries. *Mineral Processing & Extractive Metallurgy Review* 45 (8):892–903. doi: 10.1080/08827508.2024.2305382.

Krantz, P. 2023. Europe's quest for home-grown lithium. The Parliament. Accessed September 2024. https://www.theparliamentmagazine.eu/news/article/lithium-mining-race-europe-china-supply-chains .

Kumar, J., X. Shen, B. Li, H. Liu, and J. Zhao. 2020. Selective recovery of Li and $FePO_4$ from spent $LiFePO_4$ cathode scraps by organic acids and the properties of the regenerated $LiFePO_4$. *Waste Management* 113:32–40. doi: 10.1016/j.wasman.2020.05.046.

Kumari, R., and S. R. Samadder. 2022. A critical review of the pre-processing and metals recovery methods from e-wastes. *Journal of Environmental Management* 320:115887. doi: 10.1016/j.jenvman.2022.115887.

Levenspiel, O. 1999. *Chemical reaction engineering*, 3rd ed. New York, USA: John Wiley & Sons, Inc.

Li, L., J. Ge, F. Wu, R. Chen, S. Chen, and B. Wu. 2009. Recovery of cobalt and lithium from spent lithium-ion batteries using organic citric acid as leachant. *Journal of Hazardous Materials* 176 (1–3):288–93. doi: 10.1016/j.jhazmat.2009.11.026.

Li, P., S. Luo, L. Zhang, Q. Liu, Y. Wang, Y. Lin, C. Xu, J. Guo, P. Cheali, and X. Xia. 2024a. Progress, challenges, and prospects of spent lithium-ion batteries recycling: A review. *Journal of Energy Chemistry* 89:144–71. doi: 10.1016/j.jechem.2023.10.012.

Li, Y., L. Dong, P. Shi, Z. Ren, and Z. Zhou. 2024b. Selective recovery of lithium iron phosphate. *Journal of Power Sources* 598:234158. doi: 10.1016/j.jpowsour.2024.234158.

Mahandra, H., and A. Ghahreman. 2021. A sustainable process for selective recovery of lithium as lithium phosphate from spent $LiFePO_4$ batteries. *Resources, Conservation & Recycling* 175:105883. doi: 10.1016/j.resconrec.2021.105883.

Natarajan, S., A. B. Boricha, and H. C. Bajaj. 2018. Recovery of value-added products from cathode and anode material of spent lithium-ion batteries. *Waste Management* 77:455–65. doi: 10.1016/j.wasman.2018.04.032.

Nicol, M. J. 2020. The role and use of hydrogen peroxide as an oxidant in the leaching of minerals. 1. *Acid Solutions Hydrometallurgy* 193:105328. doi: 10.1016/j.hydromet.2020.105328.

Pan, S., B. Cao, D. Yuan, T. Jiao, Q. Zhang, and S. Tang. 2024. Complexes of cupric ion and tartaric acid enhanced calcium peroxide fenton-like reaction for metronidazole degradation. *Chinese Chemical Letters* 35 (7):109185. doi: 10.1016/j.cclet.2023.109185.

Paris, R., and K. V. Desboeufs. 2013. Effect of atmospheric organic complexation on iron-bearing dust solubility. *Atmospheric Chemistry & Physics* 13 (9):4895–905. doi: 10.5194/acp-13-4895-2013.

Passalacqua, J. 2023. The role of phosphates in the LFP battery supply chain. Global Markets Conference, London, UK. Accessed October 2024. https://firstphosphate.com/23-07-12%20IFA_GlobalMarketsConference.pdf.

Puigdomenech, I. 2004. Make equilibrium diagrams using sophisticated algorithms (MEDUSA). Inorganic Chemistry. Royal Institute of Technology. https://sites.google.com/site/chemdiagr/.

Punt, T., G. Akdogan, S. Bradshaw, and P. Wyk. 2021. Development of a novel solvent extraction process using citric acid for lithium-ion battery recycling. *Minerals Engineering* 173:107204. doi: 10.1016/j.mineng.2021.107204.

Reich, R., K. Slunitschek, R. M. Danisi, E. Eich, and J. Kolb. 2022. Lithium extraction techniques and the application potential of different sorbents for lithium recovery from Brines. *Mineral Processing & Extractive Metallurgy Review* 44 (4):261–80. doi: 10.1080/08827508.2022.2047041.

Saidan, M., B. Brown, and M. Valix. 2012. Leaching of electronic waste using biometabolised acids. *Journal of Chemical Engineering* 20 (3):530–34. doi: 10.1016/S1004-9541(11)60215-2.

Simeon, V. L., K. Voloder, and O. A. Weber. 1969. Complex formation in the copper(II)-tartaric acid system. *Analytica Chimica Acta* 44 (2):309–13. doi: 10.1016/S0003-2670(01)95804-0.

Sit, I., B. T. Fashina, A. P. Baldo, K. Leung, V. H. Grassian, and A. G. Ilgen. 2023. Formic acid and acetic pKa values increase under nanoconfiment. *RSC Advances* 13 (33):23147–57. doi: 10.1039/d2ra07944e.

Tian, Y., X. Ao, M. Yang, Y. Yang, J. Wei, and F. Wang. 2024. Study on the leaching of lithium from lithium-poor clay-type ore using tartaric acid by calcination and water leaching. *Hydrometallurgy* 227:106335. doi: 10.1016/j.hydromet.2024.106335.

Wang, H., G. Chen, L. Mo, G. Wu, X. Deng, and R. Cui. 2023. Recovery of Li and Co in waste lithium cobalt oxide-based battery using $H_{1.6}Mn_{1.6}O_4$. *Molecules* 28 (9):3737. doi: 10.3390/molecules28093737.

Wang, J., K. Huang, H. Dong, Y. Lu, K. Liu, Z. Chen, X. Shan, G. Huang, and L. Wei. 2022. A green process for recycling and synthesis of cathode materials $LiMn_2O_4$ from spent lithium-ion batteries using citric acid. *RSC Advances* 12 (36):23683–91. doi: 10.1039/D2RA04391B.

Wang, J., Y. Tang, and Y. Shen. 2022. Recovery of cobalt metal from waste lithium-ion batteries as sensor materials. *Sensors and Materials* 34 (6):2037–43. doi: 10.18494/SAM3746.

Zhao, T., R. Marthi, H. Mahandra, S. Chae, F. S. Traversy, Y. Choi, and A. Ghahreman. 2023. Direct selective leaching of lithium from industrial-grade black mass of waste lithium-ion batteries containing $LiFePO_4$ cathodes. *Waste Management* 171:134–42. doi: 10.1016/j.wasman.2023.08.030.

Appendix

Figure A1 shows the diffractogram of the untreated black mass sample. The presence of the lithium iron phosphate phase was confirmed ($LiFePO_4$: COD 4001849). Moreover, other species were identified, such as graphite (PDF 00-041-1487), copper and aluminium oxides (CuO: COD 9015568 and Al_2O_3: COD 5000092), and iron diphosphate ($Fe_2P_2O_7$: COD 4000291).

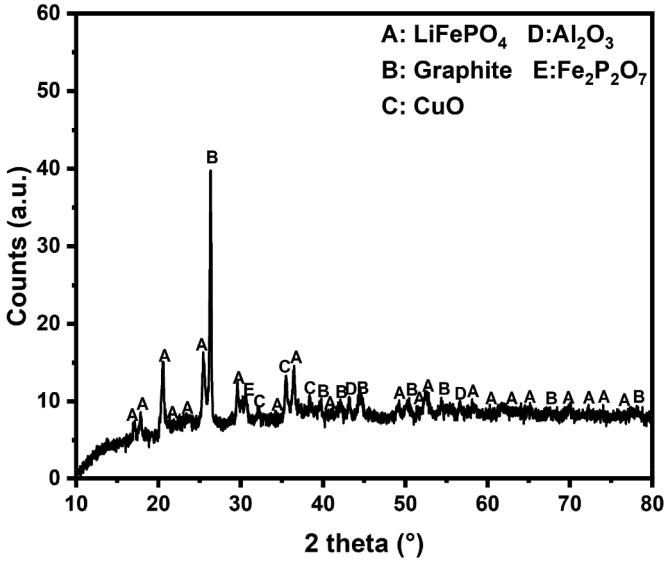

Figure A1. X-ray diffractogram of the black mass sample (original and untreated) provided by stena recycling AB company, Sweden.